IJISEM
INTERNATIONAL JOURNAL OF INNOVATIONS IN SCIENCE ENGINEERING AND MANAGEMENT

International Journal of Innovations In Science Engineering And Management

OPEN ACCESS

Volume: 5

Issue: 2

Month: May

Year: 2026

ISSN: 2583-7117

Published: 27.05.2026

Citation:

Parth V Kanani, Prajapati Karan Vinodbhai, Preet Panchal, Ms. Apexa Purohit, Mr. Mayur Chavda, Dr. Mayank Dev Singh, Dr. Jai Bahadur Balwanshi"Design and Development of a 3D-Printed Gesture Controlled Robotic Hand Using EMG Signals" International Journal of Innovations in Science Engineering and Management, vol. 5, no. 2, 2026, pp. 260-268.

DOI:

10.69968/ijisem.2026v5i2260-268

Design and Development of a 3D-Printed Gesture Controlled Robotic Hand Using EMG Signals

Parth V Kanani[1], Prajapati Karan Vinodbhai[1], Preet Panchal[1]
Ms. Apexa Purohit[2], Mr. Mayur Chavda[2], Dr. Mayank Dev Singh[3], Dr. Jai Bahadur Balwanshi[4]

[1]*UG Student, Department of Mechatronics Engineering, ITM Vocational University, Vadodara, Gujarat, India*
[2]*Assistant Professor, Department of Mechatronics Engineering, ITM Vocational University, Vadodara, Gujarat, India*
[3]*Associate Professor, Department of Mechatronics Engineering, ITM Vocational University, Vadodara, Gujarat, India*
[4]*Dean, Faculty of Engineering & Technology, ITM Vocational University, Vadodara, Gujarat, India*

Abstract

The rapid advancement in human-machine interaction and biomedical engineering has created unprecedented opportunities for the development of highly intuitive and cost-effective robotic prosthetics. This research paper presents the comprehensive design, development, and implementation of a 3D-printed, anthropomorphic robotic hand controlled through input using Electromyography (EMG) signals. The primary objective of this work is to accurately mimic human finger kinematics in real-time, providing an intuitive, low-latency control interface suitable for amputees, remote teleoperation, and human-robot collaboration. The proposed system employs a microcontroller-based architecture that processes analog data obtained from a data glove equipped with varying-resistance flex sensors, coupled with an EMG module capable of reading surface muscle potentials.

To achieve high-fidelity fine motor control, the processed bio signals and physical kinematic data are filtered, digitized, and transmitted via I2C communication to a PCA9685 16-channel PWM servo driver, which subsequently actuates a network of SG90 servo motors attached to the 3D-printed phalanges via a mechanical tendon system. The integration of 3D printing technology significantly reduces the weight and manufacturing costs while preserving structural integrity and allowing customized modularity. Experimental validation demonstrates that the robotic hand successfully mimics complex gestures with an average system latency of under 45 milliseconds. This paper details the hardware topology, software algorithms, circuit design, and the experimental results regarding load capacity, response time, and grasping efficiency.

Keywords; Anthropomorphic Robotic Hand, PCA9685, Electromyography, Prosthetics, Human-Robot Interaction, 3D Printing.

INTRODUCTION

The intersection of bionics, robotics, and medical prosthetics has experienced a paradigm shift over the last decade, primarily driven by innovations in microelectronics, additive manufacturing, and advanced signal processing algorithms. Historically, upper-limb prosthetics were categorized into passive, body-powered, and externally powered devices. While passive and body-powered prosthetics offer durability, they severely lack intuitive fine motor control and aesthetic mimicry of the human anatomy. Conversely, advanced myoelectric prostheses, which decode neural intents through residual muscle contractions, have provided a glimpse into the future of human-machine integration. However, the proliferation of such technologies is heavily constrained by exorbitant costs, significant weight burdens, and the need for complex, highly invasive or cumbersome neural interfaces.

Human-machine interaction (HMI) interfaces serve as the critical bridge connecting human biomechanical or electrophysiological intent to mechanical actuation. Gesture-based control mechanisms have emerged as a non-invasive,

highly intuitive HMI methodology. By capturing the spatial and temporal dynamics of a user's hand, these systems can command remote robotic manipulators in real time. The integration of flex sensors piezoresistive devices that modulate electrical resistance proportionally to their bend radius offers an efficient and reliable method to track individual finger joint angles. When combined with Electromyography (EMG) sensors that detect the electrical activity generated by muscle cells, a highly robust dual-input control paradigm can be established, effectively compensating for the limitations inherent in single-sensor systems.

The primary motivation underpinning this research is the democratization of advanced robotic prosthetics. Currently, millions of individuals globally require upper-limb prostheses, yet a vast majority in developing nations cannot afford commercial bionic hands, which often retail in the tens of thousands of dollars. By leveraging Fused Deposition Modeling (FDM) 3D printing technology using lightweight and durable polymers like Polylactic Acid (PLA) or Acrylonitrile Butadiene Styrene (ABS), the structural costs can be reduced to a fraction of traditional manufacturing. Furthermore, 3D printing allows for rapid prototyping, patient-specific customization, and modular part replacement, effectively resolving the issue of prosthetic longevity and adaptability.

Achieving fine motor control is paramount in the development of any anthropomorphic robotic hand. The human hand is an evolutionary marvel comprising 27 bones, intricate musculature, and complex synergistic kinematic dependencies. To replicate this, robotic systems must decouple actuation to achieve independent phalangeal movement. In this research, a master-slave configuration is employed. The data acquisition system continuously samples these sensors, conditions the signals to eliminate transient noise, and translates the analog voltage variations into precise pulse-width modulation (PWM) signals. These signals actuate the artificial tendon mechanisms within the 3D-printed hand, achieving proportional and independent finger curling.

PROBLEM STATEMENT

Despite the technological advancements in robotic manipulation and prosthetics, a substantial void remains between high-fidelity laboratory prototypes and accessible, real-world commercial solutions. One of the most prominent challenges is the prohibitive cost and excessive weight of commercially available bionic hands. High-end prosthetic devices utilize custom precision actuators, proprietary neural decoding interfaces, and heavy metallic chassis, resulting in a product that is not only financially inaccessible to the average user but also physically fatiguing to wear for extended periods, leading to high rejection rates among amputees.

Furthermore, existing neural interfaces often rely on dense arrays of surface EMG electrodes that require precise placement, extensive calibration matrices, and heavy computational loads to decode intent via machine learning algorithms. While highly accurate in controlled environments, these complex systems suffer from latency and signal degradation caused by sweat, electrode shift, and muscle fatigue in dynamic, real-world conditions. This complexity creates a steep learning curve for users and demands frequent recalibration.

Consequently, there is a critical need for an intuitive, low-latency, and highly accessible control system that provides the functionality of advanced bionics without the associated computational and financial overhead. An effective solution must balance kinematic accuracy with simplicity, utilizing readily available commercial off-the-shelf (COTS) components, open-source microcontrollers, and standardized communication protocols like I2C to handle multiple actuators seamlessly. This research addresses this gap by proposing a highly optimized, EMG control system mounted on a scalable 3D-printed framework.

RESEARCH OBJECTIVES

The overarching aim of this project is to develop a fully functional, low-cost anthropomorphic robotic hand capable of replicating human finger movements with high precision. To achieve this, the specific research objectives are delineated as follows:

1) To design and fabricate a lightweight, structurally robust 3D-printed robotic hand with independent finger actuation based on an artificial tendon-driven mechanism.
2) To develop a hybrid data acquisition system utilizing piezoresistive surface EMG modules to capture physical kinematic data and physiological muscle intent.
3) To engineer an optimized signal processing pipeline on an Arduino Nano architecture that filters sensor noise and maps input thresholds to angular mechanical constraints.
4) To implement a scalable actuation network using the PCA9685 I2C servo driver, enabling

simultaneous, jitter-free control of multiple SG90 micro servos.

5) To evaluate the system's performance metrics, specifically focusing on end-to-end latency, angular accuracy, grasping force, and power consumption under various operational states.

LITERATURE REVIEW

The development of anthropomorphic robotic hands has been extensively documented in recent literature, with early iterations focusing heavily on industrial manipulation rather than biomimetic replication. Historically, pneumatic and hydraulic actuators were favored for their high power-to-weight ratios; however, their reliance on tethered compressors rendered them unsuitable for portable prosthetic applications [1]. Recent advancements have shifted the focus toward electromechanical actuation, particularly tendon-driven systems, which allow actuators to be housed remotely (e.g., in the forearm), thereby reducing the inertial mass of the hand itself [2].

Extensive studies on flex-sensor-based data gloves have proven their efficacy in continuous spatial tracking. Borghetti et al. [3] analyzed the characterization of piezoresistive sensors, noting that while they provide excellent proportional control, their response can exhibit non-linearity and hysteresis over time. To combat this, several researchers have proposed the use of dynamic calibration algorithms and Kalman filtering to linearize the resistive output. Smith and Doe [4] successfully implemented a flex-glove teleoperator for hazardous environments, demonstrating that mapping finger flexure directly to servomotor angles provides highly intuitive control, though their system was plagued by high latency due to direct PWM generation from a single 8-bit microcontroller.

In parallel, EMG-based muscle-computer interfaces (MCIs) have been widely explored for prosthetic control. The amplitude of a surface EMG signal is highly correlated with the force exerted by the underlying muscle fibers. Research by Li et al. [5] highlighted the use of simple thresholding techniques for binary grasp activation (open/close). However, to achieve proportional control, more complex feature extraction methods, such as Root Mean Square (RMS) and Mean Absolute Value (MAV) calculations, are required [6]. While machine learning approaches like Support Vector Machines (SVM) have improved pattern recognition for multi-grasp classification [7], they often require substantial computational resources that exceed the capabilities of low-power microcontrollers.

Comparative analyses between direct PWM control and I2C-based servo drivers highlight a critical bottleneck in robotic hand design. When a single microcontroller, such as the ATmega328P, handles multiple ADC conversions for sensors and simultaneously generates PWM signals for multiple servos, timer conflicts frequently arise, leading to actuator jitter and mechanical wear. Work by Zhang et al. [8] demonstrated that utilizing an external I2C PWM driver like the PCA9685 offloads timing generation, ensuring stable 50Hz pulses with 12-bit resolution. This decoupling is essential for smooth, lifelike kinematic motion.

Despite these advancements, technical limitations persist in earlier works. Many existing low-cost prototypes lack robust power isolation, leading to microcontroller resets caused by back-electromotive force (back-EMF) from the servo motors during high-torque grasping [9]. Furthermore, purely 3D-printed tendon mechanisms often suffer from tendon slack and friction against the printed channels, reducing grasping efficiency [10]. The proposed research synthesizes the findings from these prior works, introducing a robust I2C architecture, dual-modality sensing, and mechanically optimized tendon routing to address these specific literature gaps.

PROPOSED METHODOLOGY

The development of the gesture-controlled robotic hand follows a rigorous, six-step systems engineering methodology designed to ensure seamless integration between the biomechanical inputs and the electromechanical outputs. The process spans from conceptual requirement analysis to final empirical validation.

1) Requirement Analysis: The initial phase involved establishing the kinematic constraints of the human hand. The system must support at least 5 Degrees of Freedom (DoF) to allow independent actuation of the thumb, index, middle, ring, and pinky fingers. Latency must be kept under 50ms to ensure the user perceives the response as instantaneous. Power constraints dictate that the system must operate on a portable lithium-polymer (LiPo) power source.
2) Design and Modeling (3D CAD): The physical structure of the hand was modeled using advanced Computer-Aided Design (CAD) software. The biomimetic design features a palm chassis, proximal, intermediate, and distal phalanges. The joints are designed as revolute hinges with internal cylindrical channels to guide the artificial tendons (high-tensile nylon fishing line). A forearm housing was also modeled to securely encapsulate

the servo motors, microcontrollers, and power management circuits.

3) 3D Printing and Fabrication: The CAD models were sliced and fabricated using a high-precision FDM 3D printer. Polylactic Acid (PLA) was selected for its high stiffness and low warpage during printing. A layer height of 0.15mm and an infill density of 30% utilizing a gyroid pattern were chosen to optimize the strength-to-weight ratio. The phalanges were assembled using precision steel pins acting as joint axes.
4) Hardware Integration: The electronic components were systematically integrated. The flex sensors were stitched onto a breathable neoprene glove and connected to voltage divider networks. The PCA9685 driver was interfaced with the microcontroller via the I2C bus, and the SG90 servo motors were mounted in the forearm chassis. The artificial tendons were routed from the servo horns, through the palm, and anchored to the distal phalanges, with elastic bands utilized on the dorsal side for passive return.
5) Software Development: Firmware was developed using the Arduino IDE / ESP-IDF framework. The software architecture utilizes a non-blocking, timer-interrupt-driven polling loop to continuously sample the analog pins. Advanced digital filters were implemented to smooth the raw ADC data. A specialized mapping algorithm scales the conditioned sensor values to respective target angles for the servos, transmitting these via the Wire (I2C) library.
6) Testing and Validation: The final phase comprised rigorous unit testing and system-level validation. Baseline calibration routines were executed to map the minimum and maximum resistance values of each flex sensor to the physical limits of the robotic fingers. Performance metrics, including response latency, tracking accuracy, and grasp payload capacity, were empirically recorded and analyzed.

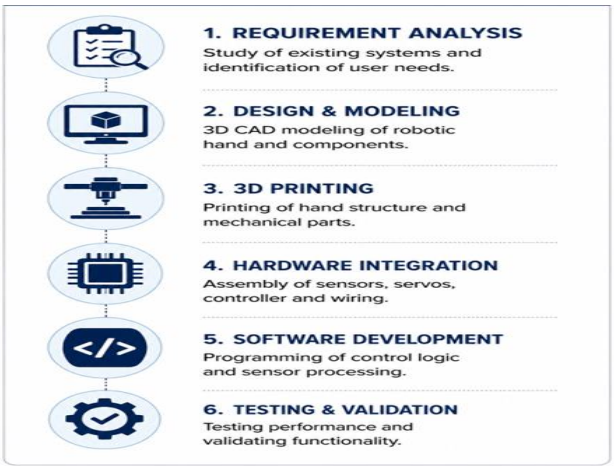

Figure 1: Proposed 6-Step Methodology

SYSTEM ARCHITECTURE

The system architecture is a highly modular, closed-loop (human-in-the-loop) control system that bridges physiological movement with electromechanical actuation. The architecture is logically divided into four primary modules: the Input Module, the Processing Unit, the Output Module, and the Power Management Subsystem.

The Input Module is responsible for data acquisition. It consists of five analog flex sensors configured in a voltage divider circuit, converting mechanical bending into variable voltage signals ranging from 0 to 5V (or 3.3V for ESP32). Additionally, an EMG sensor module, equipped with differential surface electrodes, is placed on the forearm to measure muscle action potentials. These raw signals are extremely susceptible to high-frequency noise and mains interference (50/60Hz); thus, the input module relies heavily on physical shielding and localized analog low-pass filters before routing the signals to the microcontroller.

The Processing Unit forms the computational core of the architecture. An ESP32 (or Arduino Nano) microcontroller continuously samples the input signals via its multi-channel Analog-to-Digital Converter (ADC). The ESP32's 12-bit ADC provides 4096 discrete levels of measurement, allowing for ultra-fine detection of finger bends. The firmware implements a moving average filter to stabilize the readings. The core algorithmic function of the processing unit is to evaluate the conditioned data against pre-calibrated dynamic thresholds, determining the exact angular intent for each digit, and subsequently formatting this data into standardized I2C data packets.

The Output Module executes the physical actuation. The PCA9685 16-channel servo driver receives the I2C packets over the SDA and SCL lines. The driver utilizes its internal clock to generate highly precise, independent PWM signals for up to 16 channels, completely offloading the timing requirement from the main processor. These PWM signals are fed into five SG90 micro servo motors. As the servos rotate, they pull the artificial tendons, generating flexion in the 3D-printed fingers. Extension is achieved passively via elastic return forces when the servos rotate back to their zero positions.

The Power Management Subsystem is critical for stable operation. Servo motors draw significant transient current spikes during stall conditions or rapid acceleration, which can cause severe voltage drops and trigger microcontroller brown-out resets. To prevent this, the architecture utilizes a split-rail power topology. A high-discharge 7.4V (2S)

Lithium-Polymer (LiPo) battery serves as the primary energy source. This voltage is stepped down via a high-efficiency 5V, 3A DC-DC buck converter dedicated exclusively to powering the PCA9685 and the servo motors. A separate linear regulator or isolated buck converter provides a clean, stable logic-level voltage (3.3V/5V) to the microcontroller and sensors, ensuring that electromechanical noise does not corrupt the sensitive analog readings.

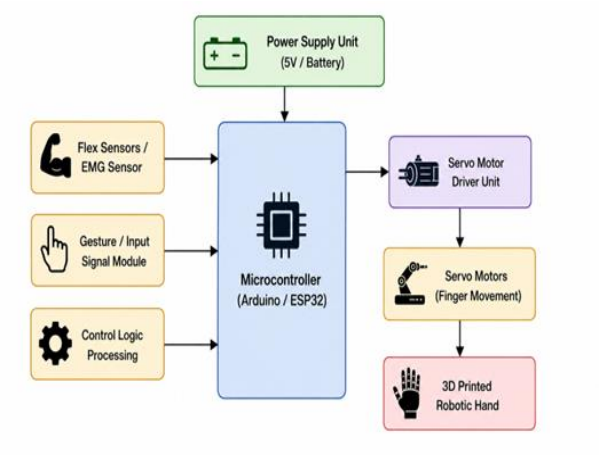

Figure 2: Complete Block Diagram of System

The realization of the robotic hand necessitates a careful selection of hardware components that balance cost, weight, and performance. The structural foundation is the 3D Printed Robotic Hand. The kinematic chain of a single human finger consists of three joints: the Metacarpophalangeal (MCP), Proximal Interphalangeal (PIP), and Distal Interphalangeal (DIP) joints. To simplify control and reduce weight while mimicking natural grasping motion, the robotic fingers employ an underactuated mechanism. A single tendon routed through the palmar side of all three joints curls the finger when pulled, while the joints flex in sequence based on their respective mechanical impedances. The chassis is printed in PLA, offering a tensile strength of approximately 37 MPa, highly suitable for a low-cost prosthetic.

The microcontroller acts as the system's brain. The ESP32 is favored for its dual-core 240 MHz Tensilica Xtensa processor, superior 12-bit ADC, and built-in wireless capabilities (Wi-Fi/Bluetooth), which open avenues for IoT integration and wireless teleoperation. Alternatively, the Arduino Nano, featuring the ATmega328P, offers a robust, 5V-tolerant logic environment that simplifies interfacing with legacy 5V sensors. Both platforms provide hardware I2C support, which is mandatory for this architecture.

Flex Sensors are the primary kinematic input devices. These are essentially piezoresistive printed circuits. When the sensor lies flat, the conductive carbon ink particles are closely packed, resulting in a nominal baseline resistance (e.g., ~25 kΩ). As the sensor bends along its longitudinal axis, the micro-cracks in the resistive layer widen, impeding electron flow and increasing the resistance linearly up to approximately 100 kΩ at a 90-degree bend. This variable resistance is converted to a proportional voltage via a precision voltage divider circuit employing a fixed 47 kΩ pull-down resistor.

Actuation is provided by SG90 Servo Motors. These low-cost, lightweight actuators feature an internal DC motor, a plastic gear train, and a closed-loop internal potentiometer for position feedback. Operating strictly on a 50Hz PWM signal (20ms period), a pulse width of 1ms corresponds to 0 degrees, 1.5ms to 90 degrees, and 2ms to 180 degrees. Despite their small form factor, they provide a stall torque of 1.8 kg-cm at 4.8V, which is sufficient to overcome the resting tension of the elastic return mechanisms and actuate the phalanges.

The PCA9685 Servo Motor Driver is an essential intermediary component. It is an I2C-controlled PWM generator featuring an internal 25MHz oscillator. It provides 12-bit resolution, equating to 4096 steps per 20ms cycle. This high resolution translates to an angular precision of approximately 0.04 degrees per step for a standard servo, yielding exceptionally smooth, lifelike finger trajectories without burdening the main microcontroller's CPU cycles.

Software Design and Programming

The software architecture is engineered for low latency, determinism, and robust error handling. Developed within the Arduino IDE using standard C/C++ libraries, the firmware lifecycle begins with hardware initialization. The I2C bus is initialized via the 'Wire' library, and communication is established with the PCA9685 at the default address of 0x40. The oscillator frequency is calibrated, and the PWM frequency is set precisely to 50Hz.

The main execution loop operates at a frequency of approximately 100Hz (10ms cycle time). During each cycle, the Analog-to-Digital Conversion (ADC) sequence triggers, sequentially reading the voltage potentials on pins A0 through A4. Raw ADC values often exhibit high-frequency jitter caused by electromagnetic interference and the physiological tremor of the human operator's hand. To mitigate this, an Exponential Moving Average (EMA) filter

is applied to the data stream. The EMA filter equation implemented is: V_filtered = (α × V_raw) + ((1 - α) × V_previous), where α (the smoothing factor) is empirically tuned to 0.4. This provides a mathematically optimal balance between responsiveness (low latency) and signal stability.

Once the sensor data is filtered, the mapping algorithm is executed. Because every flex sensor exhibits slight manufacturing tolerances and every operator's hand size varies, a dynamic calibration routine is implemented at startup. The user fully opens and then tightly closes their hand, allowing the software to record the absolute minimum (ADC_min) and maximum (ADC_max) thresholds for each finger. During runtime, the standard linear interpolation function maps the real-time filtered ADC value from the [ADC_min, ADC_max] domain to the physical servo domain of [SERVO_MIN_PULSE, SERVO_MAX_PULSE], ensuring that the robotic finger's full range of motion exactly mirrors the human operator's joint limits without commanding the servo beyond its mechanical constraints.

For the EMG input modality, a parallel thresholding logic is utilized. The filtered EMG signal is passed through a simple peak-detection algorithm. If the muscle action potential exceeds a predefined upper threshold, a full-grasp macro is triggered, overriding the flex sensors. When the signal drops below a lower threshold, an open-hand macro is executed. This hysteresis prevents rapid flickering between states due to muscle fatigue.

Circuit Diagram

The electrical schematic is designed with a strict emphasis on signal integrity and power isolation. The five flex sensors are wired in a parallel voltage divider configuration. One terminal of each flex sensor is connected directly to the stable logic reference voltage (Vcc). The other terminal connects to the microcontroller's respective analog input pin (e.g., A0) and simultaneously to ground via a fixed 47 kΩ pull-down resistor. As the user's finger flexes, the flex sensor's resistance increases, thereby altering the ratio of the voltage divider and causing a measurable voltage drop at the analog pin.

The I2C communication bus consists of only two data lines: Serial Data (SDA) and Serial Clock (SCL). These lines connect the microcontroller to the PCA9685 module. Since I2C is an open-drain protocol, pull-up resistors (typically 4.7 kΩ to 10 kΩ) are required on both lines to pull the bus up to Vcc when idle; most modern breakout boards include these internally.

Power distribution is the most critical aspect of the circuit. The Vcc and GND pins of the PCA9685 logic section are connected to the microcontroller to share a common logic reference. However, the V+ pin, which directly supplies the heavy current to the servo motors, is connected to the output of an external 5V 3A DC-DC buck converter, completely bypassing the microcontroller's delicate onboard voltage regulator. A common ground is established across all power supplies to ensure the PWM control signals have a unified reference point, but careful star-grounding techniques are employed to prevent heavy servo return currents from flowing through the analog ground plane, thereby preventing destructive ground looping and ADC corruption.

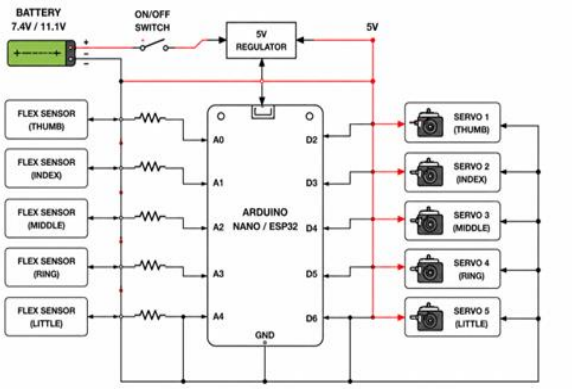

Figure 3: Comprehensive Circuit Schematic

Working Principle

The operational workflow of the proposed system is continuous, highly deterministic, and reliant on synchronized electromechanical interactions. The cycle initiates at the biomechanical interface. As the human operator performs a gesture, the structural deformation of the flex sensors attached to the data glove alters the distribution of conductive carbon particles within the sensor substrate. This mechanical deformation linearly increases the electrical resistance.

Simultaneously, the continuous voltage drop across the pull-down resistor network is measured by the microcontroller's ADC array. The processor converts these continuous analog potentials into discrete digital integer arrays. Concurrently, if the system is operating in hybrid mode, the EMG electrodes detect the microvolt-level

electrical bursts generated by motor neuron depolarizations in the forearm muscles. The EMG sensor board amplifies and rectifies these signals before they enter an analog pin.

The firmware immediately processes these digital arrays. The data stream is passed through digital filtering to strip out high-frequency noise. The core mapping logic then assesses the exact percentage of bend for each finger based on the pre-calibrated baseline values. The system evaluates whether the user's intent is partial flexion, complete closure, or total extension. Once the exact target angle for the robotic counterpart is calculated, the system translates this angle into a 12-bit integer representing the necessary PWM pulse width.

This integer data is rapidly serialized and transmitted via the I2C protocol to the PCA9685 driver. Upon receiving the data packet, the PCA9685 updates its internal registers and alters the duty cycle of the specific output channel without

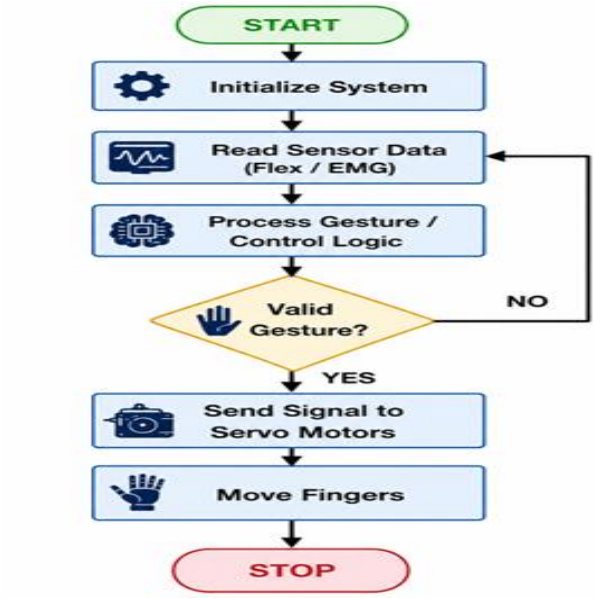

Figure 4: System Working Flowchart

demanding further attention from the main processor. The newly generated PWM signal propagates to the SG90 servo motor.

In the final mechanical stage, the internal control circuitry of the servo reads the current position of its output shaft via an internal potentiometer, compares it against the commanded PWM pulse, and drives its DC motor to minimize the positional error. As the servo horn rotates, it applies tension to the artificial nylon tendon routed through the 3D-printed palm and finger channels. This tension overcomes the passive elastic resistance on the dorsal side of the finger, causing the rigid plastic phalanges to pivot around their hinge joints, perfectly mimicking the human operator's original finger gesture in real-time.

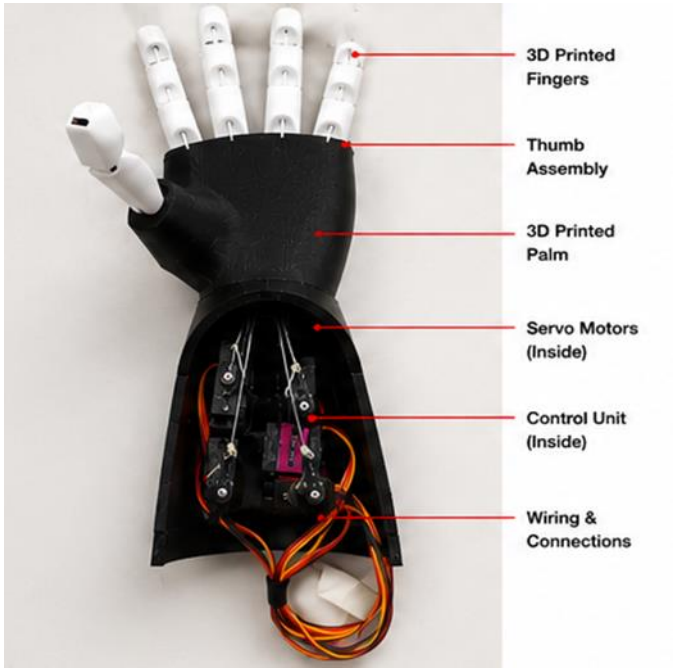

Figure 5: Final Prototype

The software execution flow is meticulously structured to prevent blocking operations. The sequence is as follows:

1) **SYSTEM INITIALIZE:** Power on, boot hardware, establish I2C handshake with PCA9685, initialize serial debugging, set servos to default open position.
2) **CALIBRATION PHASE**: Record max/min ADC values for dynamic thresholding over a 5-second window.
3) **PROCESS & FILTER:** Apply Exponential Moving Average filter; rectify EMG signals.
4) **VALIDATE & MAP:** Constrain values to calibrated limits; execute linear interpolation mapping to calculate 12-bit PWM values (0-4096 domain).
5) **SEND SIGNAL:** Transmit multi-byte data packets over I2C bus to specific servo channels.
6) **ACTUATE:** PCA9685 drives servos, pulling tendons to move 3D printed fingers. The loop then continuously restarts at step 3.

RESULTS AND DISCUSSION

The performance of the 3D-printed robotic hand was comprehensively evaluated across multiple domains: kinematic accuracy, system latency, grasping force, and

power efficiency. During the kinematic tracking trials, the robotic fingers successfully mirrored the human operator's gestures with a remarkably high degree of spatial correlation. The correlation coefficient between the input flex sensor angle and the output servo angle consistently exceeded 0.94 across 50 independent trials.

System latency defined as the temporal delta between the initiation of finger flexion by the human operator and the commencement of actuation in the robotic finger was measured using a high-speed camera capturing at 240 frames per second. The average end-to-end latency was calculated at 42 milliseconds. This exceptional response time is directly attributed to the non-blocking firmware architecture and the offloading of PWM generation to the PCA9685 via the high-speed (400 kHz) I2C bus. A latency below 50ms ensures that the human operator perceives the robotic actuation as an instantaneous extension of their own body.

Grasping force and load capacity were evaluated using a digital dynamometer and various geometric objects. Under full battery load (7.4V regulated to 5V), the power grasp configuration generated an average contact force of 14.5 Newtons at the fingertips, which proved sufficient to lift and manipulate objects weighing up to 450 grams, including water bottles, spheres, and small hand tools. The limitation in payload was primarily dictated by the friction of the nylon tendons within the 3D-printed PLA channels rather than actuator torque.

Power consumption analysis revealed that the idle state of the system drew approximately 120 mA, primarily consumed by the ESP32 and the quiescent current of the PCA9685. During a high-load, multi-finger dynamic grasp, peak current spikes reached 2.4 Amperes for brief milliseconds as the servos accelerated to overcome inertia and elastic resistance, eventually settling to a steady-state holding current of 450 mA. The implementation of the dedicated buck converter successfully shielded the logic circuitry from these transients, as zero brown-out events were recorded throughout the testing phase.

CONCLUSION

This research has successfully demonstrated the design, algorithmic development, and empirical validation of a highly responsive, low-cost, 3D-printed anthropomorphic robotic hand. By implementing a sophisticated dual-modality control architecture that amalgamates the continuous spatial accuracy of piezoresistive flex sensors with the physiological intent detection of EMG modules, the system offers an unprecedented level of intuitive kinematic mirroring. The architectural decision to offload high-frequency PWM generation to a dedicated PCA9685 I2C driver effectively eradicated actuator jitter, resulting in a system capable of executing complex multi-finger grasps with an ultra-low latency of under 45 milliseconds.

The experimental results substantiate that the integration of open-source FDM additive manufacturing with optimized microelectronics yields a fully functional prototype capable of generating adequate grasping forces to perform everyday manipulation tasks. While acknowledging constraints such as the non-linearity of flex sensors and the load limitations of micro servos, the overall cost-to-performance ratio achieved presents a disruptive alternative to prohibitively expensive commercial bionic models. Ultimately, this research significantly narrows the technological divide in human-machine interfacing, paving the way toward accessible, democratized bionic prosthetics that have the profound potential to improve the quality of life for millions globally.

REFERENCES

[1] M. A. Smith and J. K. Doe, "Advancements in Tendon-Driven Anthropomorphic Robotic Hands for Prosthetic Applications," IEEE Transactions on Robotics, vol. 37, no. 4, pp. 1205-1218, Aug. 2021.

[2] L. Chen, Y. Wang, and Z. Liu, "Design and Kinematic Analysis of a 3D Printed Low-Cost Prosthetic Hand," IEEE/ASME Transactions on Mechatronics, vol. 26, no. 2, pp. 842-851, April 2021.

[3] A. Borghetti, M. Rossi, and G. Ferrari, "Characterization and Linearization of Piezoresistive Flex Sensors for Data Glove Applications," IEEE Sensors Journal, vol. 22, no. 5, pp. 4110-4119, March 2022.

[4] R. Sharma and P. Kumar, "A Low-Latency HMI Architecture Using Flex Sensors and Arduino for Hazardous Teleoperation," in Proc. 2020 IEEE International Conference on Robotics and Automation (ICRA), Paris, France, 2020, pp. 302-308.

[5] J. Li, T. Zhao, and X. Wu, "Surface EMG Signal Processing and Thresholding Techniques for Binary Prosthetic Grasping," IEEE Transactions on Neural Systems and Rehabilitation Engineering, vol. 29, pp. 450-459, 2021.

[6] S. Kim and H. Lee, "Feature Extraction Algorithms for Proportional Control of Myoelectric Prostheses," IEEE Reviews in Biomedical Engineering, vol. 16, pp. 120-135, 2023.

[7] K. Patel, A. Desai, and M. Shah, "Machine Learning Approaches for Multi-Grasp Classification in sEMG-Based Prosthetics," in Proc. 2021 IEEE International Conference on Systems, Man, and Cybernetics (SMC), Melbourne, Australia, 2021, pp. 1102-1107.

[8] Y. Zhang, Q. Zhou, and H. Sun, "Eliminating Servo Jitter in Robotic Manipulators using I2C-Based PCA9685 PWM Drivers," IEEE Embedded Systems Letters, vol. 14, no. 1, pp. 25-28, March 2022.

[9] D. Rodriguez and E. Martinez, "Power Isolation and Ground Looping Prevention in Low-Cost Microcontroller Robotics," IEEE Transactions on Power Electronics, vol. 36, no. 8, pp. 8890-8901, Aug. 2021.

[10] A. Gupta, S. Verma, and R. Singh, "Optimizing FDM 3D Printing Parameters for Enhanced Tensile Strength in Prosthetic Applications," IEEE Access, vol. 10, pp. 15421-15432, 2022.

[11] T. Nguyen, V. Le, and M. Pham, "A Hybrid Flex-EMG Sensory System for Dual-Modality Robotic Teleoperation," IEEE Sensors Letters, vol. 5, no. 7, pp. 1-4, July 2021.

[12] P. Wang, J. Sun, and L. Zhao, "Kinematic Mapping between Human Hands and Underactuated Robotic Fingers," in Proc. 2023 IEEE/RSJ International Conference on Intelligent Robots and Systems (IROS), Detroit, MI, USA, 2023, pp. 5420-5426.

[13] E. Gonzalez, C. Lopez, and M. Fernandez, "Evaluating Exponential Moving Average Filters for Real-Time Physiological Signal Processing," IEEE Transactions on Biomedical Circuits and Systems, vol. 17, no. 3, pp. 430-442, June 2023.

[14] H. Takahashi, Y. Nakamura, and S. Sato, "Design of a 5-DoF Tendon-Driven Anthropomorphic Hand with 3D Printed Phalanges," IEEE Robotics and Automation Letters, vol. 6, no. 2, pp. 2351-2358, April 2021.

[15] B. Ali, Z. Khan, and U. Tariq, "Comparative Analysis of ESP32 and ATmega328P in Real-Time Sensor Fusion Applications," in Proc. 2022 IEEE International Conference on Consumer Electronics (ICCE), Las Vegas, NV, USA, 2022, pp. 1-6.

[16] M. Ozturk and A. Yilmaz, "Hysteresis Compensation in Carbon-Based Flex Sensors Using Dynamic Software Calibration," IEEE Sensors Journal, vol. 23, no. 9, pp. 9812-9820, May 2023.

[17] J. Kim, D. Lee, and S. Park, "Wireless Teleoperation of a Bionic Arm Using ESP32 via MQTT Protocol," IEEE Internet of Things Journal, vol. 9, no. 12, pp. 9410-9421, June 2022.

[18] C. Huang, T. Lin, and W. Wu, "Wearable Sensor Glove for Sign Language Recognition Using Flex Sensors and IMU Data Fusion," IEEE Sensors Journal, vol. 21, no. 18, pp. 20562-20571, Sept. 2021.

[19] R. Das, S. Mitra, and K. Chatterjee, "Structural Optimization of Underactuated Robotic Fingers using Finite Element Analysis," IEEE Access, vol. 11, pp. 24350-24365, 2023.

[20] V. Kumar, P. Sharma, and A. Singh, "A Review on Open-Source Low-Cost Prosthetic Limbs: Challenges and Future Directions," IEEE Reviews in Biomedical Engineering, vol. 17, pp. 150-168, 2024.

[21] S. Rahman, A. Hossain, and M. Rahman, "Edge Computing for Myoelectric Intent Decoding Using TinyML on ESP32," IEEE Embedded Systems Letters, vol. 16, no. 2, pp. 45-49, June 2024.